Composites: Part B 42 (2011) 444–455

Contents lists available at ScienceDirect

Composites: Part B

journal homepage: www.elsevier.com/locate/compositesb

Equivalent electro-elastic properties of Macro Fiber Composite (MFC) transducers using asymptotic expansion approach

Fabio Biscani [a,b,c], Houssein Nasser [a,*], Salim Belouettar [a], Erasmo Carrera [b]

[a] Centre de Recherche Public Henri Tudor, 29, Avenue John F. Kennedy, L-1855 Luxembourg, Luxembourg
[b] Department of Aerospace Engineering, Politecnico di Torino, Torino, Italy
[c] Institut Jean le Rond d'Alembert, UMR 7190, CNRS UNIV Paris 06, Paris, France

ARTICLE INFO

Article history:
Received 23 July 2010
Received in revised form 7 December 2010
Accepted 9 December 2010
Available online 22 December 2010

Keywords:
A. Ceramic-matrix composites
A. Smart materials
B. Electrical properties
Asymptotic Expansion Homogenization

ABSTRACT

This paper aims to model and compute the effective electro-mechanical properties of Macro Fiber Composite (MFC) transducers using the Asymptotic Expansion Homogenization (AEH) method. The AEH method is commonly used to solve problems involving physical phenomena on continuous media with periodic micro-structures. In particular, the AEH is a useful technique to study the behaviour of structural components built with composite materials. The obtained results are satisfactory when compared with those obtained using the Periodic Homogenization Method (PHM) as well as with the experimental results available from the literature.

1. Introduction

Piezoelectricity is the ability of some materials to convert an electric stimulus into mechanical energy, and vice versa. Piezoelectric materials are currently being used in a number of applications such as submarine hydrophones, accelerometers, microphones, ultrasonic devices, and electronic resonators. Piezoelectric Fibre Composites called Active Fibre Composite (AFC) were introduced by Hagood and Bent [1] as an alternative to monolithic piezoceramic wafers for structural actuation applications. AFCs actuators and sensors offer many advantages over conventional monolithic piezoceramic devices. The multiphase construction yields a more robust actuator that is capable of being added to complex surface shapes. When equipped with interdigitated electrodes (IDEs) [2–4], AFCs are more responsive than with conventional electrodes. Developed by the NASA-Langley Research Center, the Macro Fiber Composite (MFC) actuator and sensor present superior qualities among AFCs in performance, behaviour and repeatability as well as in manufacturability [5], and thus attracted great interest for new industrial applications and in the academic community as well. While the MFC's attributes render it an exceptionally useful device, limited modelling and experimental characterisation research on the MFC has took place. Among these studies, Williams et al. [6] have analyzed experimentally the nonlinear tensile and shear stress–strain behaviour and Poisson effects of the MFC. Williams et al. [7] have later developed a nonlinear model for a piezoelectric continuum taking into account nonlinear mechanical behaviour and actuation characteristic of MFC.

In the last decade, an increasing number of investigations focused on the homogenisation of composite materials have been accomplished to predict mechanical and electro-mechanical properties of piezoceramic composites. Different techniques have been developed, such as analytical mixing rules [4,8,9] and finite element modelling techniques [10–13]. Hagood and Bent [1] used a mixing rule technique to predict the effective properties of AFCs. The results of this investigation were in reasonable agreement with experimental data. Moreover, Bent and Hagood [4] adopted the Uniform Field Method (UFM) to derive a constitutive model for a new AFC design. The model was implemented into a finite element code and numerical simulations have been performed. In [8,9], Tan and Tong proposed three-dimensional micro-electromechanical models for piezoelectric fibre reinforced composite materials. Analytical formulas of overall electro-mechanical properties have been derived using the UFM under single and multiple loads conditions. The developed model showed good agreement with experimental data. Using similar approach, Deraemaeker et al. [14,15] proposed a simplified form of the analytical mixing rules based on the work of Tan and Tong [8]. The results of the investigated simplified analytical solution have shown a good agreement with the numerical solution computed using the Periodic Homogenization Method [10,16] under plane stress assumption and with the experimental results available in literature. In [17,18], homogenisation techniques based on Eshelby tensor [19] have been developed to predict the mechanical and coupled piezoelectric properties of composites. In the same context, Li [20] considered the Mori–

* Corresponding author.
E-mail address: houssein.nasser@tudor.lu (H. Nasser).

1359-8368/$ - see front matter © 2010 Elsevier Ltd. All rights reserved.
doi:10.1016/j.compositesb.2010.12.009

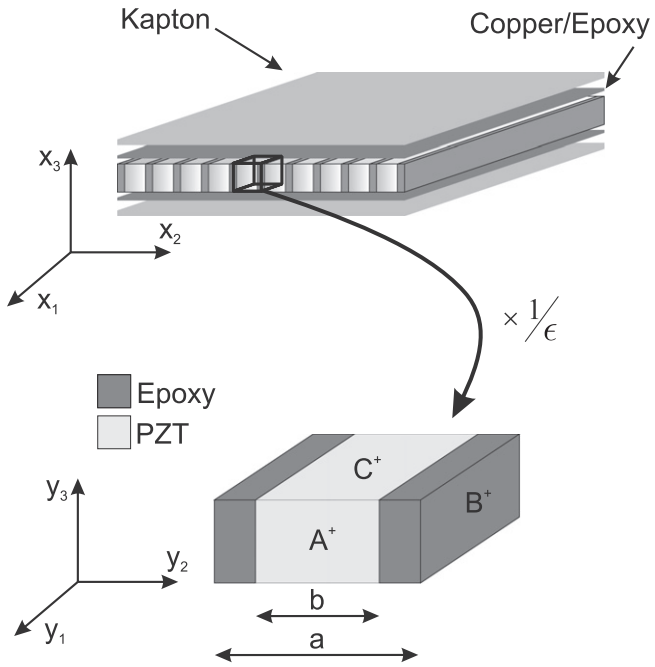

Fig. 1. MFC d_{31}. According to Smart Materials datasheets, Kapton layers thickness is 0.04 mm, copper/epoxy layers thickness is 0.0018 mm and active layer thickness is 0.18 mm. The RVE of the active layer is depicted.

Tanaka [21] and the self consistent [22] approaches to predict the effective thermoelastic moduli of composites. Koutsawa et al. [23] extended the generalised self consistent approach to estimate the electro-mechanical properties of piezocomposite.

The method of Asymptotic Expansion Homogenization (AEH) is a powerful method that allows to compute the effective properties of composite materials and heterogeneous media using a periodic Representative Volume Element (RVE). It is often used in many global/local and periodical problems. For instance, AEH method is able also to characterize the micro field of stress, strain, electric displacement and electric fields [24,25]. The AEH method for periodic media has been formulated, in a weak form derivation, by Guedes and Kikuchi [26]. Recently, a strong form derivation of the AEH for linear elasticity problems has been presented in [12,25] and applied to several composite geometries, where detailed mathematical formulation and numerical implementation for elastic properties can be found. The influence of the reinforcement volume fraction on the overall material properties for different composite geometries has also been analyzed in these works. In [27], Bravo-Castillero et al. applied AEH method to obtain the overall effective properties of periodic multi-laminated magneto-electro-elastic composites.

In this paper an attempt is made to compute the effective electro-mechanical properties of d_{31}-type MFC using the AEH method. Section 2 introduces the constitutive equations and geometric properties of the MFC. In Section 3, the AEH method is solved analytically, without considering the effect of the electrodes, and numerically considering the electrodes. In Section 4, the uniform field method is presented and the formulae of UFM are compared to those of AEH analytical solution. The Periodic Homogenization Method is considered in Section 5 as a numerical validation of the AEH. The results obtained using the different methods are presented in Section 6 and compared to the experimental results from manufacturer datasheets.

2. Preliminaries

During the machining process, after sintering, polycrystalline piezoceramics have isotropic properties at the macroscale. After the poling process, the behaviour of the piezoelectric material becomes transversally isotropic with respect to the poling direction, usually referred to as direction 3. The linear constitutive equations of piezoelectric materials involve linear coupling between stress, strain, electric field and electric displacement (or between force, displacement, electric charge and electric potential). In a Cartesian coordinate system, the subscripts 1, 2, 3, 4, 5 and 6 represent the subscripts *x*, *y*, *z*, *yz*, *xz* and *xy*, respectively. The constitutive equations for orthotropic piezoelectric materials using the notations of the *IEEE standard on piezoelectricity* are as follows:

Sensing: the direct piezoelectric effect refers to the conversion of mechanical energy into electric energy:

$$\mathbf{D} = \mathbf{eS} + \boldsymbol{\varepsilon}^{S}\mathbf{E} \tag{1}$$

Actuation: the converse piezoelectric effect refers to the conversion of electric energy into mechanical energy:

$$\mathbf{T} = \mathbf{C}^{E}\mathbf{S} - \mathbf{e}^{T}\mathbf{E} \tag{2}$$

where $\mathbf{E}$, $\mathbf{D}$ are the electric field vector and the electric displacement vector, and $\mathbf{T}$, $\mathbf{S}$ are the stress and strain vectors. $\mathbf{C^E}$, $\mathbf{e}$ and $\boldsymbol{\varepsilon}^{S}$ are respectively stiffness matrix at constant electric field, piezoelectric properties and permittivity at zero strain.

At micro-scale, piezofibre composites have a periodic geometry defined by an epoxy matrix surrounding the active fibres. To express the properties of this type of composites, a micromechanical model is defined on the basis the RVE concept. Periodic mechanical and electrical boundary conditions are required at the boundaries of the RVE. Homogeneous constitutive equations of the RVE piezocomposite are determined by the effective properties of the RVE, neglecting boundary effects at the edges of the actuator. To estimate the effective properties, volume averaging of the different fields within the RVE is used. Stress $\overline{\mathbf{T}}$, strain $\overline{\mathbf{S}}$, electric displacement $\overline{\mathbf{D}}$ and electric field $\overline{\mathbf{E}}$ are given by

$$\begin{aligned} \overline{T}_i &= \frac{1}{V}\int_V T_i \,\mathrm{d}V, \qquad \overline{S}_i = \frac{1}{V}\int_V S_i \,\mathrm{d}V, \\ \overline{D}_i &= \frac{1}{V}\int_V D_i \,\mathrm{d}V, \qquad \overline{E}_i = \frac{1}{V}\int_V E_i \,\mathrm{d}V \end{aligned} \tag{3}$$

where V is the volume of the RVE.

The constitutive equations of the homogenised RVE model are expressed as

$$\overline{\mathbf{T}} = \mathbf{C^{E^h}}\overline{\mathbf{S}} - \mathbf{e^{T^h}}\overline{\mathbf{E}} \tag{4}$$

$$\overline{\mathbf{D}} = \mathbf{e^h}\overline{\mathbf{S}} + \boldsymbol{\varepsilon}^{\mathbf{S^h}}\overline{\mathbf{E}} \tag{5}$$

where $\mathbf{C^{E^h}}$, $\mathbf{e^h}$ and $\boldsymbol{\varepsilon}^{\mathbf{S^h}}$ are respectively the effective stiffness matrix at constant electric field, the effective piezoelectric properties and the effective permittivity at zero strain of the homogeneous model.

The constitutive Eqs. (1) and (2) can be expressed as:

$$\begin{Bmatrix} T_1 \\ T_2 \\ T_3 \\ T_4 \\ T_5 \\ T_6 \\ D_1 \\ D_2 \\ D_3 \end{Bmatrix} = \underbrace{\begin{bmatrix} C^E_{11} & C^E_{12} & C^E_{13} & 0 & 0 & 0 & 0 & 0 & -e_{31} \\ C^E_{12} & C^E_{22} & C^E_{23} & 0 & 0 & 0 & 0 & 0 & -e_{32} \\ C^E_{13} & C^E_{23} & C^E_{33} & 0 & 0 & 0 & 0 & 0 & -e_{31} \\ 0 & 0 & 0 & C^E_{44} & 0 & 0 & 0 & -e_{24} & 0 \\ 0 & 0 & 0 & 0 & C^E_{55} & 0 & -e_{15} & 0 & 0 \\ 0 & 0 & 0 & 0 & 0 & C^E_{66} & 0 & 0 & 0 \\ 0 & 0 & 0 & 0 & e_{15} & 0 & \varepsilon^S_{11} & 0 & 0 \\ 0 & 0 & 0 & e_{24} & 0 & 0 & 0 & \varepsilon_{22} & 0 \\ e_{31} & e_{32} & e_{33} & 0 & 0 & 0 & 0 & 0 & \varepsilon^S_{33} \end{bmatrix}}_{\text{generalised constitutive matrix } \mathbf{C_g}} \begin{Bmatrix} S_1 \\ S_2 \\ S_3 \\ S_4 \\ S_5 \\ S_6 \\ E_1 \\ E_2 \\ E_3 \end{Bmatrix} \tag{6}$$

The left hand vector, called vector of generalised stresses ($\mathbf{T_g}$), contains the stress and the electric displacement components. The right hand vector is the vector of generalised strains ($\mathbf{S_g}$) and it contains the strain and the electric field components. The matrix $\mathbf{C_g}$ is called generalised constitutive matrix. It is built on the basis of the elastic, the piezoelectric and the dielectric properties. Fig. 1 shows the geometry of MFC d_{31}-type together with the corresponding RVE where the parameter $\rho = b/a$ represents the volume fraction of the piezoelectric phase.

3. Effective properties of MFCs using the AEH method

3.1. On the Asymptotic Expansion Homogenization method

The method of Asymptotic Expansion Homogenization (AEH) [12,24–26] is a powerful method that allows to compute the homogeneous model of composite materials and heterogeneous media through an analysis of a periodic Representative Volume Element (RVE). It is often used in many global/local and periodical problems. Loading of such materials gives periodic oscillations in the fields at microstructural level as a consequence of periodicity. Two different scales can be identified. There is a "fast" variable y over the RVE and a "slow" variable x over the structure, related through

$$y = x/\epsilon \tag{7}$$

where $\epsilon \ll 1$ is a scale parameter.

The periodicity of the RVE in the structure is assumed. The components of the generalised elasticity tensor (tensor form of the generalised constitutive matrix $\mathbf{C_g}$) is described as:

$$D_{ijkl} = D_{ijkl}(y) \tag{8}$$

The expression of the Y-periodic generalised elasticity tensor in the macroscale x is:

$$D_{ijkl}(x/\epsilon) = D^{\epsilon}_{ijkl}(x) \tag{9}$$

A generic quantity $Q(x)$, function of x and Y-periodic over the scale ϵ, is given as $Q^{\epsilon}(x)$. In the following, the generalised elasticity tensor is assumed as

$$D_{ijkl} = C^{E}_{ijkl}, \quad D_{4jkl} = e_{jkl}, \quad D_{ij4l} = e_{lij}, \quad D_{4j4l} = -\varepsilon^{s}_{jl} \tag{10}$$

with indexes varying from 1 to 3. C^{E}_{ij} are the components of the elastic modulus tensor at constant electric field; ε^{s}_{ij} are the components of the dielectric tensor at fixed strain; e_{ij} are the components of the piezoelectric constants tensor at fixed strain or electric field. In order to derive the relation of the AEH, the dimension of the RVE is assumed to be infinitesimal with respect to the structure ($\epsilon \to 0$). This allows to consider x and y as separate variables. The generalised displacement field (physical displacement and potential) is approximated using an asymptotic expansion in ϵ as:

$$u^{\epsilon}_i(x) = u^{(0)}_i(x,y) + \epsilon u_i(x,y)^{(1)} + \epsilon^2 u^{(2)}_i(x,y) + \cdots \tag{11}$$

where $u_i(x,y)^{(j)}$, with $i = 1,\ldots,4$ and $j \in N_0$, are the correctors of the generalised displacement field. Since x and y are independent variables, one can write:

$$\frac{\partial}{\partial x^{\epsilon}_i} = \frac{\partial}{\partial x_i} + \frac{1}{\epsilon}\frac{\partial}{\partial y_i} \tag{12}$$

Applying Eq. (12) to the asymptotically expanded generalised displacement field of Eq. (11), the expressions of the generalised strains and stresses is obtained as function of ϵ. Substituting these expressions into the generic Boundary Value Differential (BVD) problem and grouping the terms according to the power of ϵ, the original BVD problem can be split in a series of simpler BVD problems. The solution of this set of simpler BVD problems corresponds to the solution of the original one asymptotically (with $j \to \infty$ in Eq. (11)) if the hypothesis of this approach are verified, i.e. if the material is periodic and the dimension of the RVE tends to zero. It comes out from the third lowest order BVD that

$$D^{h}_{ijmn} = \frac{1}{|Y|}\int_Y D_{ijkl}(y)\left[I^{mn}_{kl} - \frac{\partial \chi^{mn}_k(y)}{\partial y_l}\right]\mathrm{d}y \tag{13}$$

where D^{h}_{ijmn} is the equivalent generalised elasticity tensors, Y is the domain of the RVE, $|Y|$ is the RVE volume, I^{mn}_{kl} is the identity tensor and χ^{mn}_k is called the characteristics displacement tensor that can be computed thanks to a relation derived from the two lowest order BVDs:

$$\frac{\partial}{\partial y_j}\left[D_{ijkl}(y)\left(I^{mn}_{kl} - \frac{\partial \chi^{mn}_k(y)}{\partial y_l}\right)\right] = 0 \tag{14}$$

In order to solve this equation it is necessary to consider the boundary conditions, which involves also the quantity

$$\sigma^{(1)}_{ij} = \left[D_{ijkl}(y)\left(I^{mn}_{kl} - \frac{\partial \chi^{mn}_k(y)}{\partial y_l}\right)\right]\frac{\partial u^{(0)}_m}{\partial x_n}(x) \tag{15}$$

derived from the two lowest order BVD. $\sigma^{(1)}_{ij}$ is the term multiplying ϵ^0 in the asymptotic expansion of the generalised stresses.

3.2. AEH analytical solution

Due to the simple geometry of the MFC, the material properties are given as:

$$D_{ijkl}(y_2) = \begin{cases} D^{\text{fibre}}_{ijkl} & \text{for } 0 < y_2 <= \rho|Y| \\ D^{\text{matrix}}_{ijkl} & \text{for } \rho|Y| < y_2 < |Y| \end{cases} \tag{16}$$

Eqs. (13)–(15) could be written respectively as

$$D^{h}_{ijmn} = \frac{1}{|Y|}\int_Y D_{ijk2}(y_2)\left[I^{mn}_{k2} - \frac{\partial \chi^{mn}_k(y_2)}{\partial y_2}\right]\mathrm{d}y_2 \tag{17}$$

$$\frac{\partial}{\partial y_2}\left[D_{i2k2}(y_2)\left(I^{mn}_{k2} - \frac{\partial \chi^{mn}_k(y_2)}{\partial y_2}\right)\right] = 0 \tag{18}$$

$$\sigma^{(1)}_{i2} = \left[D_{i2k2}(y_2)\left(I^{mn}_{k2} - \frac{\partial \chi^{mn}_k(y_2)}{\partial y_2}\right)\right]\frac{\partial u^{(0)}_m}{\partial x_n}(x) \tag{19}$$

where y_2 is the direction along which the material properties varies in the RVE (see Fig. 1) and $|Y|$ is the length of the RVE along y_2. Eq. (18) is a system of differential equations that can be solved as:

$$\begin{cases} \frac{\partial \chi^{mn}_{k_1}}{\partial y_2} = (D_{k2o2})^{-1}D_{o2mn} - (D_{k2o2})^{-1}K_{omn_1} & \text{for } 0 < y <= \rho|Y| \\ \frac{\partial \chi^{mn}_{k_2}}{\partial y_2} = (D_{k2o2})^{-1}D_{o2mn} - (D_{k2o2})^{-1}K_{omn_2} & \text{for } \rho|Y| < y < |Y| \end{cases} \tag{20}$$

K_{omn_1} and K_{omn_2} are constant terms. The subscript 1 stands for the fibre phase and the subscript 2 stands for the matrix phase. Hereafter, expressions such as $(D_{k2o2})^{-1}$ stand for the inverse of a bidimensional matrix. The values of K_{omn} can be obtained from the boundary conditions. Since the BCs are applied on χ^{mn}_k and on $\frac{\partial \chi^{mn}_k}{\partial y_2}$, Eq. (20) can be solved

$$\begin{cases} \chi^{mn}_{k_1}(y_2) = (D_{k2o2})^{-1}D_{o2mn}y_2 - (D_{k2o2})^{-1}K_{omn_1}y_2 + G_{kmn_1} \\ \chi^{mn}_{k_2}(y_2) = (D_{k2o2})^{-1}D_{o2mn}y_2 - (D_{k2o2})^{-1}K_{omn_2}y_2 + G_{kmn_2} \end{cases} \tag{21}$$

with G_{omn_1} and G_{omn_2} as constant terms. The BCs are considered to find the values of the constant terms K_{omn_1}, K_{omn_2}, G_{kmn_1} and G_{kmn_2} in Eq. (21):

- perfect bonding between the phases

$$\chi^{mn}_{k_1}(\rho Y) = \chi^{mn}_{k_2}(\rho Y) \tag{22}$$

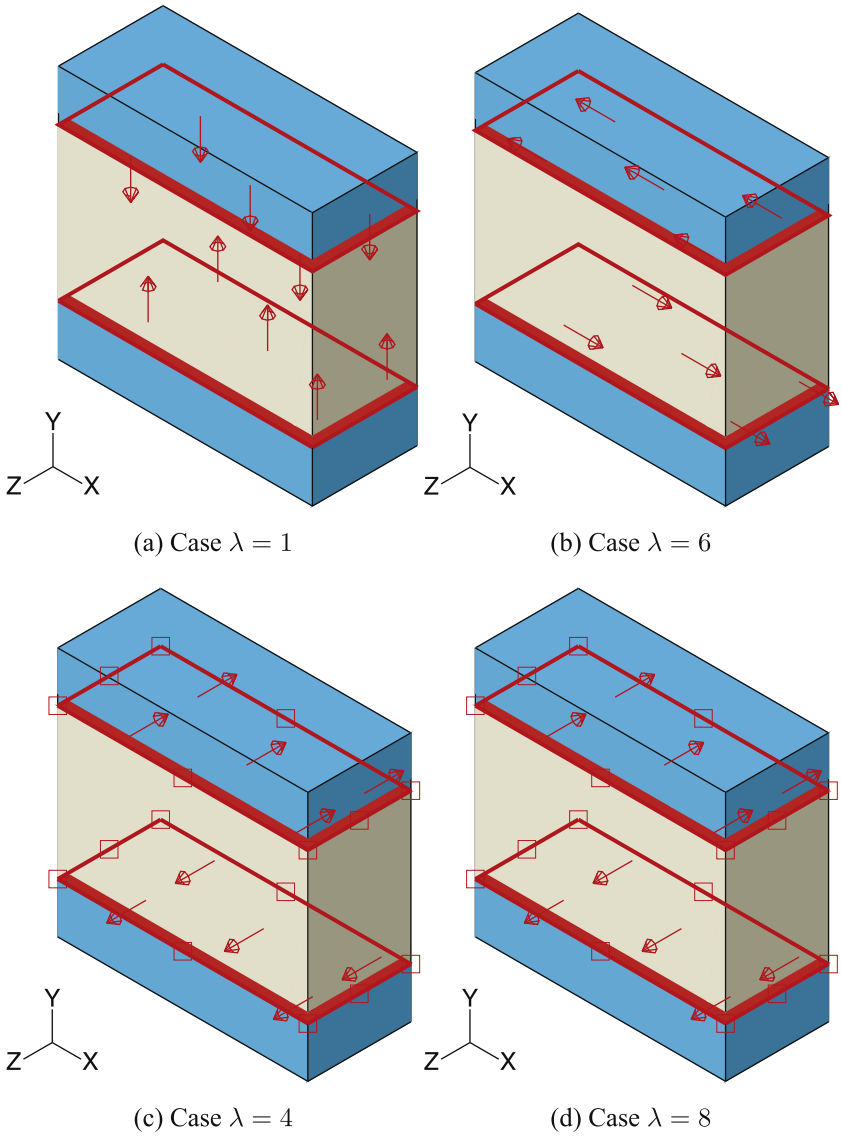

Fig. 2. Representation of the four load cases. Arrows stand for applied surface forces and squares stand for applied surface charges. Cases $\lambda = 4$ and $\lambda = 8$ differ in the magnitude of applied loads and charges (see Table 1).

- continuity of the stress between the phases

$$\sigma^{(1)}_{i2_1}(\rho Y) = \sigma^{(1)}_{i2_2}(\rho Y) \tag{23}$$

- Y-periodicity

$$\chi^{mn}_{k_1}(0) = \chi^{mn}_{k_2}(Y) \tag{24}$$
$$\sigma^{(1)}_{i2_1}(0) = \sigma^{(1)}_{i2_2}(Y) \tag{25}$$

- unicity condition, i.e. zero average on Y

$$\overline{\chi^{mn}_k} = \frac{1}{|Y|}\int_Y \chi^{mn}_k(y_2)\mathrm{d}y_2 = 0 \tag{26}$$

As a matter of fact, only $K_{omn_1} = K_{omn_2} = K_{omn}$ is needed to compute the equivalent properties

$$K_{omn} = \left(\overline{(D_{o2p2})^{-1}}\right)^{-1}\overline{(D_{p2q2})^{-1}D_{q2mn}} \tag{27}$$

where the operator $\overline{\bullet}$ performs an average over the RVE:

$$\overline{X} = \frac{1}{|Y|}\int_Y X(y_2)\mathrm{d}y_2 \tag{28}$$

Substituting Eq. (27) in Eq. (20):

$$\frac{\partial \chi^{mn}_k}{\partial y_2} = (D_{k2o2})^{-1}D_{o2mn} - (D_{k2o2})^{-1}\left(\overline{(D_{o2p2})^{-1}}\right)^{-1}\overline{(D_{p2q2})^{-1}D_{q2mn}} \tag{29}$$

The equivalent properties for the AEH can be computed with the substitution of Eq. (29) in Eq. (17):

$$D^h_{ijmn} = \overline{D_{ijmn}} - \overline{D_{ijk2}(D_{k2o2})^{-1}D_{o2mn}} + \left(\overline{D_{ijk2}(D_{k2o2})^{-1}(D_{o2p2})^{-1}}\right)^{-1}\overline{(D_{p2q2})^{-1}D_{q2mn}} \tag{30}$$

3.3. AEH numerical solution

The analytical solution for the AEH could be obtained since the material properties vary only in one direction, leading to a 1D homogenisation problem. However, this is not sufficient to take

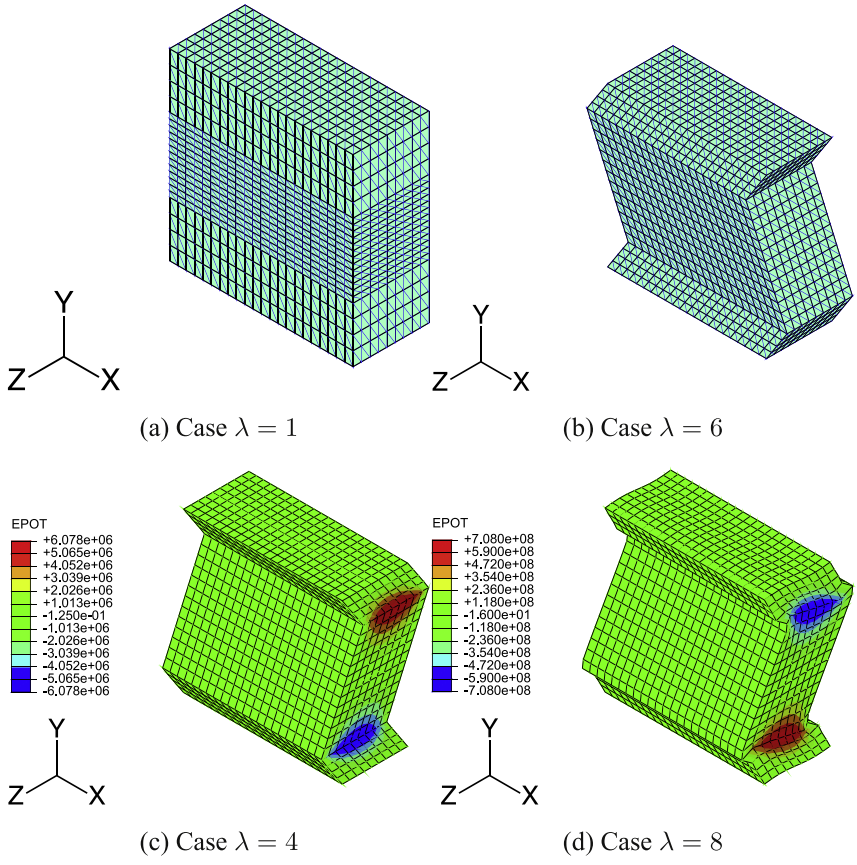

Fig. 3. Deformed RVE. Colormap represents the electric potential distribution. In the cases $\lambda = 1$ and $\lambda = 6$ the electric potential is uniform.

into account the electrodes. To overcome this limitation a 3D homogenisation model has been developed. The equations to be considered are Eqs. (13) and (14), here rewritten for convenience:

$$D^h_{ijmn} = \frac{1}{|Y|}\int_Y D_{ijkl}(y)\left[I^{mn}_{kl} - \frac{\partial \chi^{mn}_k(y)}{\partial y_l}\right]\mathrm{d}y \tag{31}$$

$$\frac{\partial}{\partial y_j}\left[D_{ijkl}(y)\left(I^{mn}_{kl} - \frac{\partial \chi^{mn}_k(y)}{\partial y_l}\right)\right] = 0 \tag{32}$$

In order to calculate the effective properties with Eqs. (31) and (32) have to be solved. This is equivalent to solving the following auxiliary variational problem:

$$\int_Y D_{ijkl}\frac{\partial \chi^{mn}_k}{\partial y_l}\frac{\partial v_i}{\partial y_j}\,\mathrm{d}Y = \int_Y D_{ijmn}\frac{\partial v_i}{\partial y_j}\,\mathrm{d}Y, \quad v_i \in V_Y \tag{33}$$

$\chi^{mn}_k \in V_Y$, where V_Y is the set of Y-periodic continuous and sufficiently regular functions with zero average value in Y [25]. This problem is similar to a electro-mechanical one in which χ^{mn}_k is the generalised displacement field. It is solved using FEM. Details about how to enforce the periodicity of χ^{mn}_k can be found in [12]. It can be derived that the right-hand side of Eq. (33) corresponds to generalised surface loads acting at interfaces between different materials, with direction and module dependent on the material properties jump across the interface. It can be stated that these loads ensures the fulfilment of the boundary conditions in Eq. (23). In fact the continuity of χ^{mn}_k across the material interfaces is guaranteed by the finite element model but the continuity of the physical stress of Eq. (15) is enforced through a discontinuity in the "mathematical" stress of the mechanical-like problem of Eq. (33).

In the piezoelectric case, given a 9×9 generalised constitutive matrix $\mathbf{C_g}$ (matrix form of the tensor D_{ijmn}), each column corresponds to a particular load case. If the interface among the different materials has a normal vector

$$\vec{\mathbf{n}} = (n_1, n_2, n_3) \tag{34}$$

and the orthonormal system of vectors is $\vec{\mathbf{i}}_1,\ \vec{\mathbf{i}}_2,\ \vec{\mathbf{i}}_3$ then:

$$\begin{aligned}\vec{\mathbf{F}} = {} & \Delta C_{g1\lambda} n_1 \vec{\mathbf{i}}_1 + \Delta C_{g2\lambda} n_2 \vec{\mathbf{i}}_2 + \Delta C_{g3\lambda} n_3 \vec{\mathbf{i}}_3 + \Delta C_{g4\lambda} n_2 \vec{\mathbf{i}}_3 + \Delta C_{g4\lambda} n_3 \\ & \times \vec{\mathbf{i}}_2 + \Delta C_{g5\lambda} n_1 \vec{\mathbf{i}}_3 + \Delta C_{g5\lambda} n_3 \vec{\mathbf{i}}_1 + \Delta C_{g6\lambda} n_1 \vec{\mathbf{i}}_2 + \Delta C_{g6\lambda} n_2 \vec{\mathbf{i}}_1\end{aligned} \tag{35}$$

$$Q = \Delta C_{g7\lambda} n_1 + \Delta C_{g8\lambda} n_2 + \Delta C_{g9\lambda} n_3$$

$\vec{\mathbf{F}}$ is a surface mechanical load and Q is a surface electrical charge. λ is an index that corresponds to a couple m, n, i.e to a column of matrix $\mathbf{C_g}$. In the case of MFC the interface between the two phases is perpendicular to y_2. Therefore $n_1 = n_3 = 0$ and $n_2 = 1$ and Eq. (35) become:

$$\vec{\mathbf{F}} = \Delta C_{g2\lambda} n_2 \vec{\mathbf{i}}_2 + \Delta C_{g4\lambda} n_2 \vec{\mathbf{i}}_3 + \Delta C_{g6\lambda} n_2 \vec{\mathbf{i}}_1 \tag{36}$$

$$Q = \Delta C_{g8\lambda} n_2 \tag{37}$$

In the RVE model there are two interfaces that have opposite signs for a given applied surface mechanical load or surface charge. Because of the orthotropy of the materials of the MFC, only seven load cases could be considered instead of nine. Load cases are presented in Table 1. Four of these, namely $\lambda = 1, 2, 3, 9$, differ only in the magnitude of the applied loads. Thanks to the linearity of the problem only four load cases out of seven need to be solved and the other three load cases are computed with a simple ratio. A graphical representation of the load cases is given in Fig. 2. The RVE is meshed with 1300 8-node brick piezoelectric elements using commercial FEM software ABAQUS. A mesh convergence analysis has been

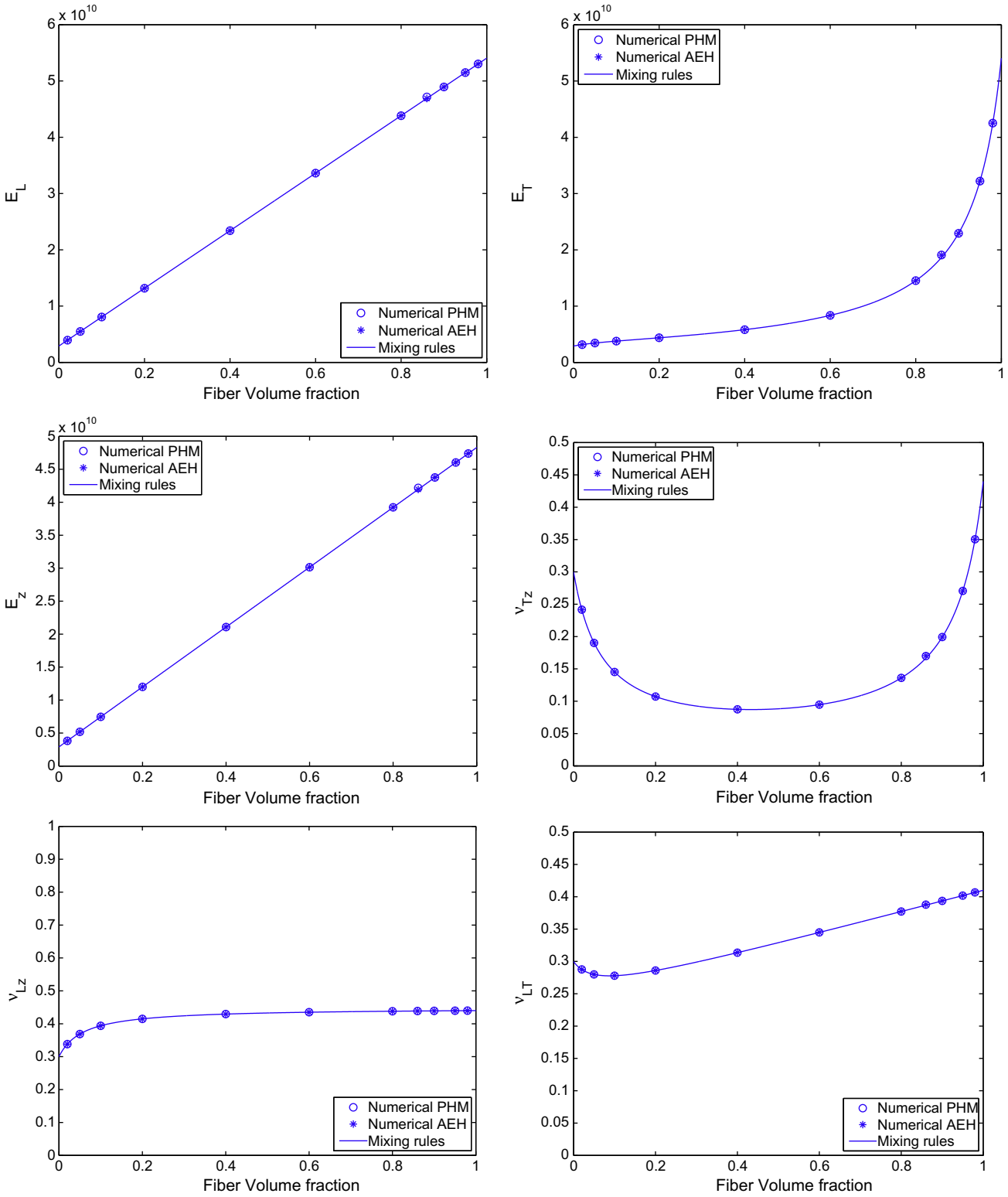

Fig. 4. Computed mechanical properties of d_{31} MFC as a function of fibre volume fraction ρ. Elastic moduli are in Pa.

performed. The adopted mesh guarantees the convergence of at least three significant digits of the computed equivalent material properties. In ABAQUS Theory Manual [28] it is shown that the part of the generalised load vector corresponding to applied charges has a negative sign. Although this is correct for the physical piezoelectric problem, it is not valid for the variational problem of AEH. Therefore, surface charges in Eqs. (35) and (37) must be changed of sign. Moreover, during the postprocessing phase, in which the effective properties are computed via Eq. (31), the signs of the electric field components given by the FEM solver must be changed due to the definition of the electric field as the gradient of the electric potential changed of sign. The problem can be numerically ill conditioned for the load cases that correspond to $\lambda = 8$ and $\lambda = 9$ because of the small entity of the applied generalised loads. A

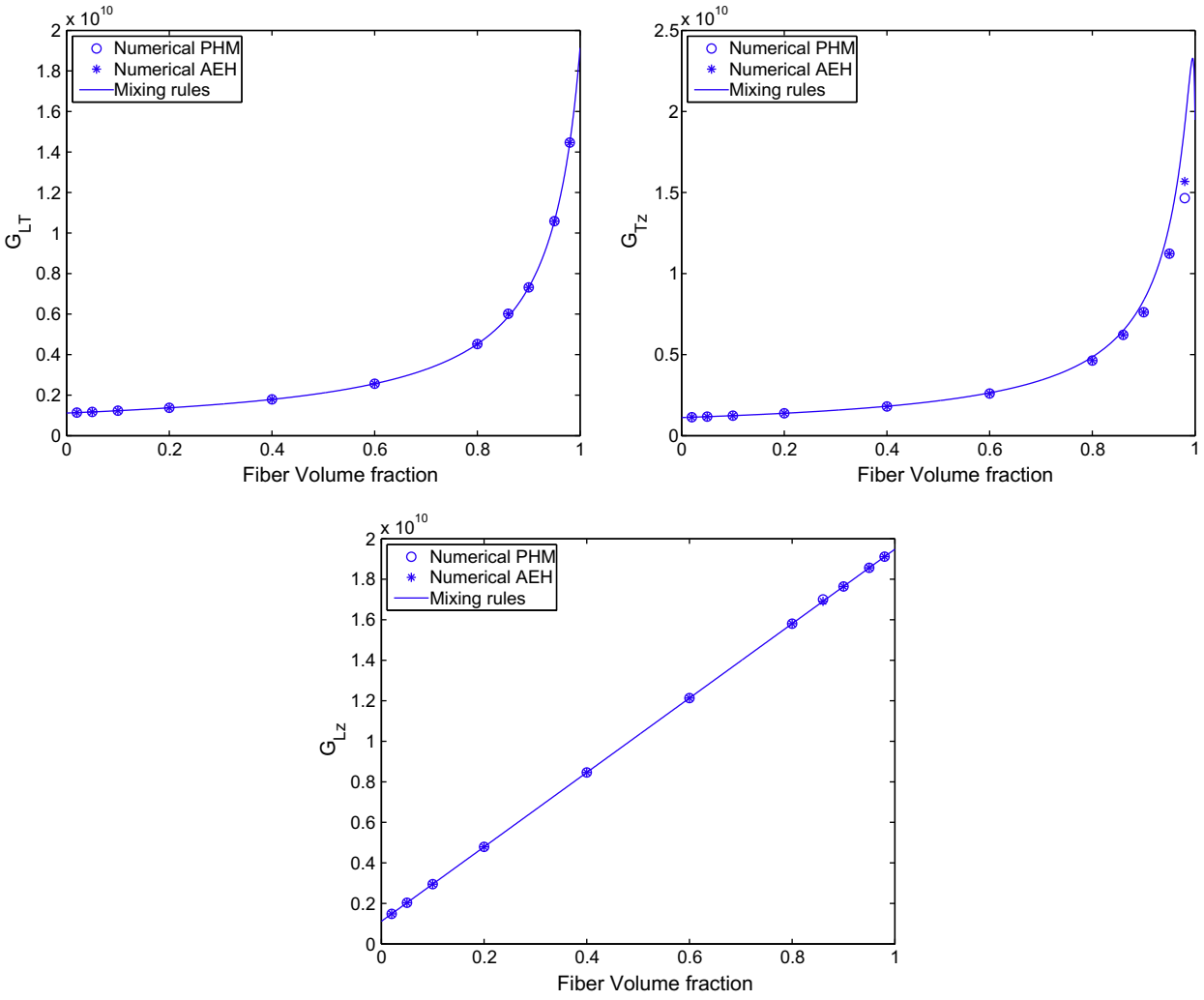

Fig. 5. Computed mechanical properties of d_{31} MFC as a function of fibre volume fraction ρ. Results are in Pa.

simple solution is to magnify the loads by a factor that will be used in the postprocessing phase to scale the FEM results. Without electrodes the results correspond to the analytical solution found in Section 3.2. This does not apply when electrodes are considered. This is performed imposing a constant zero electrical potential on the electrodes surface via boundary conditions. Fig. 3 shows the deformed RVE for the four load cases together with the colormap of the electric potential distribution.

4. Uniform field method

The uniform field method (UFM) [4,8,14] is adopted to obtain analytical formulae for the equivalent properties of the MFC in order to make a comparison with the analytical AEH solution reported in Eq. (30). UFM is based on the hypothesis that fields such as stress fields and strain fields are uniform in each phase of the RVE. At this stage the relations among fields, which are necessary to derive the effective properties, are presented.

4.1. Relationships among fields

The effective properties derived with the UFM depends on the relationships among fields in the RVE as a whole and in the phases. These relationships depend on the geometry of the RVE and derive directly from the uniform field hypothesis. In the case of a two phase piezoelectric composite, relationships among the fields can be of either of the following form:

- in the case of independent variable, the fields are equal in each constituent:

$$\overline{X_i} = X_i^p = X_i^m \tag{38}$$

- in the case of dependent variable, the fields are related through a linear mixture relation:

$$\overline{X_i} = \rho X_i^p + (1-\rho) X_i^m \tag{39}$$

where ρ is the volume fraction of the piezoelectric phase. $\overline{X_i}$ is a generic generalised stress or strain for the whole RVE (mean value); X_i^p is its value in the piezoelectric phase and X_i^m is its value in the matrix phase. Corresponding generalised stress and strain have different kinds of relationships, i.e. if $\overline{T_1} = T_1^p = T_1^m$ then $\overline{S_1} = \rho S_1^p + (1-\rho) S_1^m$.

Each generalised stress or strain has its own relationship among fields. In the case of MFC, provided that y_2 is the direction along which the materials properties change (see Fig. 1), S_1, S_3, S_5, E_1 and E_3 are independent, whereas S_2, S_4, S_6 and E_2 are dependent. Stress and electric displacement components are dependent or independent accordingly.

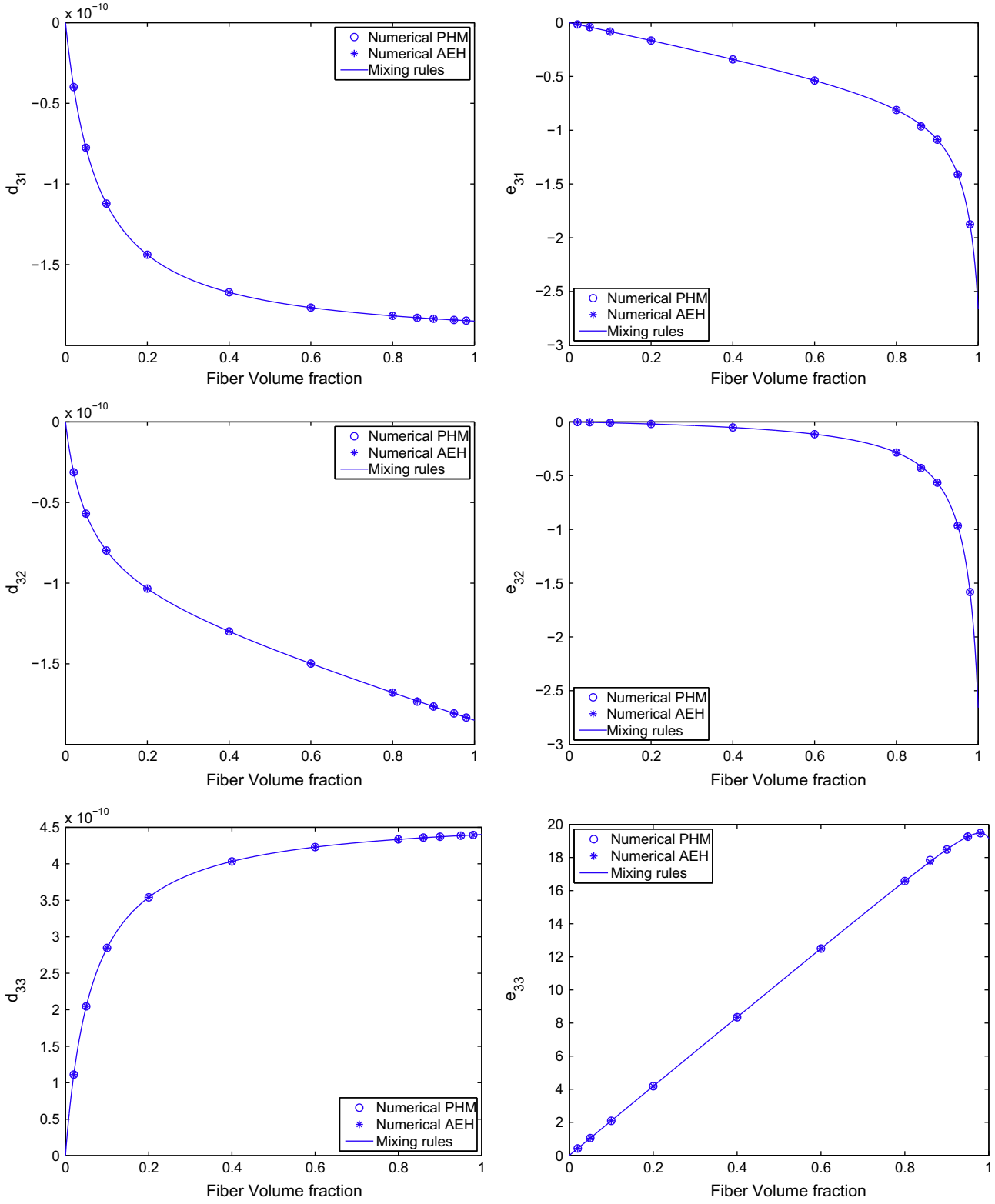

Fig. 6. Computed strain piezoelectric constants d and stress piezoelectric constants e of d_{31} MFC as a function of fibre volume fraction ρ. d components are given in C/N, e components are given in C/m^2.

4.2. Matrix-based procedure

A matrix-based procedure is implemented in a symbolic manipulation software to obtain the formulae for the equivalent properties and in a numerical software to obtain the values of the equivalent properties. Due to this approach lengthy and error prone manual computations are avoided. The procedure is based on the partition of the vector of generalised stresses $\mathbf{T_g}$, the generalised constitutive matrix $\mathbf{C_g}$ and the vector of generalised strains $\mathbf{S_g}$ according to the dependency or independency property of each

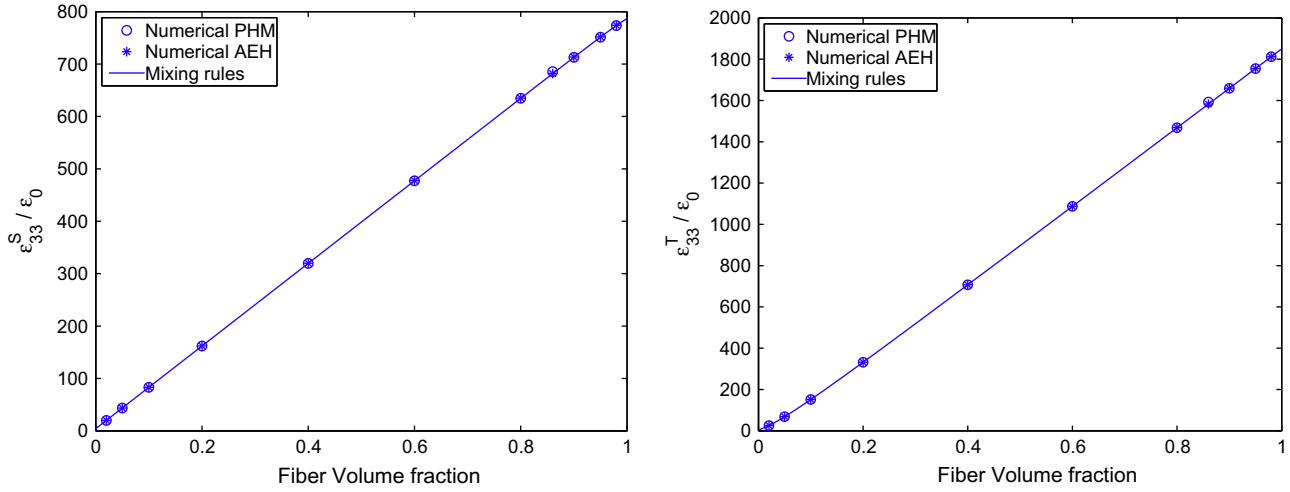

Fig. 7. Computed dielectric constants of d_{31} MFCs as a function of fibre volume fraction ρ at zero strain (left) and at free strain (right).

Table 1
Applied surface loads and surface charges to the RVE in numerical AEH.

Case	Surface force			Surface charge
	y_1 component	y_2 component	y_3 component	
$\lambda = 1$	$F_1 = 0$	$F_2 = \Delta C_{g21}$	$F_3 = 0$	$Q = 0$
$\lambda = 2$	$F_1 = 0$	$F_2 = \Delta C_{g22}$	$F_3 = 0$	$Q = 0$
$\lambda = 3$	$F_1 = 0$	$F_2 = \Delta C_{g23}$	$F_3 = 0$	$Q = 0$
$\lambda = 4$	$F_1 = 0$	$F_2 = 0$	$F_3 = \Delta C_{g44}$	$Q = \Delta C_{g84}$
$\lambda = 6$	$F_1 = \Delta C_{g66}$	$F_2 = 0$	$F_3 = 0$	$Q = 0$
$\lambda = 8$	$F_1 = 0$	$F_2 = 0$	$F_3 = \Delta C_{g48}$	$Q = \Delta C_{g88}$
$\lambda = 9$	$F_1 = 0$	$F_2 = \Delta C_{g29}$	$F_3 = 0$	$Q = 0$

generalised stress and strain. The procedure is divided into a series of steps:

1. Rearrangement of Eq. (6) separating dependent and independent generalised stresses and strains

$$\begin{Bmatrix} \{\mathbf{T}_I\} \\ \{\mathbf{T}_D\} \end{Bmatrix} = \begin{bmatrix} [\mathbf{C}_{II}] & [\mathbf{C}_{ID}] \\ [\mathbf{C}_{DI}] & [\mathbf{C}_{DD}] \end{bmatrix} \times \begin{Bmatrix} \{\mathbf{S}_I\} \\ \{\mathbf{S}_D\} \end{Bmatrix} \tag{40}$$

   where $[\mathbf{C}_{II}]$, $[\mathbf{C}_{DI}]$, $[\mathbf{C}_{ID}]$, $[\mathbf{C}_{DD}]$ can be derived from $\mathbf{C}$ with row and column permutations, according to the rearrangement of $\mathbf{T}$ and $\mathbf{S}$.
2. Extraction of the dependent variables in terms of the independent ones:

$$\begin{Bmatrix} \{\mathbf{T}_D\} \\ \{\mathbf{S}_D\} \end{Bmatrix} = \begin{bmatrix} [\mathbf{A}_1] & [\mathbf{A}_2] \\ [\mathbf{A}_3] & [\mathbf{A}_4] \end{bmatrix} \times \begin{Bmatrix} \{\mathbf{T}_I\} \\ \{\mathbf{S}_I\} \end{Bmatrix} \tag{41}$$

   The vector on the left hand side is called $\{\mathbf{X}\}_D$ and the vector on the right-hand side is called $\{\mathbf{X}\}_I$. It can be shown that

$$[\mathbf{A}_1] = [\mathbf{C}_{DD}][\mathbf{C}_{ID}]^{-1} \tag{42}$$
$$[\mathbf{A}_2] = [\mathbf{C}_{DI}] - [\mathbf{C}_{DD}][\mathbf{C}_{ID}]^{-1}[\mathbf{C}_{II}] \tag{43}$$
$$[\mathbf{A}_3] = [\mathbf{C}_{ID}]^{-1} \tag{44}$$
$$[\mathbf{A}_4] = -[\mathbf{C}_{ID}]^{-1}[\mathbf{C}_{II}] \tag{45}$$

   and the matrix containing $\mathbf{A}_1$, $\mathbf{A}_2$, $\mathbf{A}_3$ and $\mathbf{A}_4$ is called $\mathbf{A}$.
3. According to the boundary conditions in Eq. (39)

$$\{\overline{\mathbf{X}}\}_D = \rho\{\mathbf{X}\}_D^f + (1-\rho)\{\mathbf{X}\}_D^m \tag{46}$$

where the superscript f stands for the piezoelectric phase and the superscript m for the matrix phase. According to Eq. (41), Eq. (46) can be written as

$$\left[\mathbf{A}^h\right]\{\overline{\mathbf{X}}\}_I = \rho\left[\mathbf{A}^f\right]\{\mathbf{X}\}_I^f + (1-\rho)\left[\mathbf{A}^m\right]\{\mathbf{X}\}_I^m \tag{47}$$

where the superscript h stands for homogeneous. Because of the boundary conditions in Eq. (38), Eq. (47) can be simplified as:

$$\left[\mathbf{A}^h\right] = \rho\left[\mathbf{A}^f\right] + (1-\rho)\left[\mathbf{A}^m\right] \tag{48}$$

4. Equivalent properties can be obtained from A^e. Inverting Eqs. (42)–(45) one can get:

$$\left[\mathbf{C}_{ID}^h\right] = \left[\mathbf{A}_3^h\right]^{-1} \tag{49}$$
$$\left[\mathbf{C}_{DD}^h\right] = \left[\mathbf{A}_1^h\right]\left[\mathbf{C}_{ID}^h\right] \tag{50}$$
$$\left[\mathbf{C}_{II}^h\right] = -\left[\mathbf{C}_{ID}^h\right]\left[\mathbf{A}_4^h\right] \tag{51}$$
$$\left[\mathbf{C}_{DI}^h\right] = \left[\mathbf{A}_2^h\right] + \left[\mathbf{C}_{DD}^h\right]\left[\mathbf{A}_3^h\right]\left[\mathbf{C}_{II}^h\right] \tag{52}$$

The output of this calculation is the matrix $\mathbf{C}_\mathbf{g}^h$, which contains in each element the formula to evaluate the corresponding equivalent property or its value. For example in the first row, first column, if a symbolic manipulation software is used there is the formula to evaluate the equivalent C_{11}. If a numerical software is used there is the value of the equivalent C_{11}. Formulae to evaluate equivalent properties of anisotropic materials can become very lengthy. Error prone manual computations are avoided with the presented procedure. In order to implement it $\mathbf{C_{ID}}$ and $\mathbf{A}_3^h$ must be invertible. $\mathbf{C_{ID}}$ in the case of the MFC is considered in Appendix A.

4.3. Equivalence between UFM and AEH for MFCs

Expressions for the Equivalent properties in Eq. (30) obtained using AEH method correspond exactly to the formulae derived according to the UFM in the case of the MFC. Eq. (29) is considered in order to understand this equivalence. It should be stated that:

- $\frac{\partial \chi_k^{mn}}{\partial y_2}$ is piecewise constant, depending only on the material properties that are piecewise constant.

- Integrating $\frac{\partial \chi_k^{mn}}{\partial y_2}$ in y_2, χ_k^{mn} can be computed. It is piecewise linear in y_2 and is independent of y_1, y_3.

The displacement, strain and stress fields obtained with the AEH method are considered. In the AEH method, the first order approximation of the generalised displacement field (see Eq. (11)) is expressed as:

Table 2
Periodic boundary conditions for PHM: u^i_{jK} is the displacement in direction j in the ith node of the face K, φ^i_K is the electric potential in the ith node of the face K, q is an arbitrary non-null value.

Case	Mechanical and electrical BC			Computed coefficients
	A^+ and A^-	B^+ and B^-	C^+ and C^-	
1	$u^i_{1A^+} - u^i_{1A^-} = q$ $\varphi^i_{A^+} - \varphi^i_{A^-} = 0$	$u^i_{2B^+} - u^i_{2B^-} = 0$ $\varphi^i_{B^+} - \varphi^i_{B^-} = 0$	$u^i_{3C^+} - u^i_{3C^-} = 0$ $\varphi^i_{C^+} - \varphi^i_{C^-} = 0$	$C^E_{11}, C^E_{21}, C^E_{31}, e_{31}$
2	$u^i_{1A^+} - u^i_{1A^-} = 0$ $\varphi^i_{A^+} - \varphi^i_{A^-} = 0$	$u^i_{2B^+} - u^i_{2B^-} = q$ $\varphi^i_{B^+} - \varphi^i_{B^-} = 0$	$u^i_{3C^+} - u^i_{3C^-} = 0$ $\varphi^i_{C^+} - \varphi^i_{C^-} = 0$	$C^E_{12}, C^E_{22}, C^E_{32}, e_{32}$
3	$u^i_{1A^+} - u^i_{1A^-} = 0$ $\varphi^i_{A^+} - \varphi^i_{A^-} = 0$	$u^i_{2B^+} - u^i_{2B^-} = 0$ $\varphi^i_{B^+} - \varphi^i_{B^-} = 0$	$u^i_{3C^+} - u^i_{3C^-} = q$ $\varphi^i_{C^+} - \varphi^i_{C^-} = 0$	$C^E_{13}, C^E_{23}, C^E_{33}, e_{33}$
4	$u^i_{1A^+} - u^i_{1A^-} = 0$ $\varphi^i_{A^+} - \varphi^i_{A^-} = 0$	$u^i_{3B^+} - u^i_{3B^-} = q$ $\varphi^i_{B^+} - \varphi^i_{B^-} = 0$	$u^i_{2C^+} - u^i_{2C^-} = q$ $\varphi^i_{C^+} - \varphi^i_{C^-} = 0$	C^E_{44}, e_{24}
5	$u^i_{3A^+} - u^i_{3A^-} = q$ $\varphi^i_{A^+} - \varphi^i_{A^-} = 0$	$u^i_{2B^+} - u^i_{2B^-} = 0$ $\varphi^i_{B^+} - \varphi^i_{B^-} = 0$	$u^i_{1C^+} - u^i_{1C^-} = q$ $\varphi^i_{C^+} - \varphi^i_{C^-} = 0$	C^E_{55}, e_{15}
6	$u^i_{2A^+} - u^i_{2A^-} = q$ $\varphi^i_{A^+} - \varphi^i_{A^-} = 0$	$u^i_{1B^+} - u^i_{1B^-} = q$ $\varphi^i_{B^+} - \varphi^i_{B^-} = 0$	$u^i_{3C^+} - u^i_{3C^-} = 0$ $\varphi^i_{C^+} - \varphi^i_{C^-} = 0$	C^E_{66}
7	$u^i_{1A^+} - u^i_{1A^-} = 0$ $\varphi^i_{A^+} - \varphi^i_{A^-} = 0$	$u^i_{2B^+} - u^i_{2B^-} = 0$ $\varphi^i_{B^+} - \varphi^i_{B^-} = 0$	$u^i_{3C^+} - u^i_{3C^-} = 0$ $\varphi^i_{C^+} - \varphi^i_{C^-} = q$	$\varepsilon^S_{33}, e_{31}, e_{32}, e_{33}$
8	$u^i_{1A^+} - u^i_{1A^-} = 0$ $\varphi^i_{A^+} - \varphi^i_{A^-} = 0$	$u^i_{2B^+} - u^i_{2B^-} = 0$ $\varphi^i_{B^+} - \varphi^i_{B^-} = q$	$u^i_{3C^+} - u^i_{3C^-} = 0$ $\varphi^i_{C^+} - \varphi^i_{C^-} = 0$	$\varepsilon^S_{22}, e_{24}$
9	$u^i_{1A^+} - u^i_{1A^-} = 0$ $\varphi^i_{A^+} - \varphi^i_{A^-} = q$	$u^i_{2B^+} - u^i_{2B^-} = 0$ $\varphi^i_{B^+} - \varphi^i_{B^-} = 0$	$u^i_{3C^+} - u^i_{3C^-} = 0$ $\varphi^i_{C^+} - \varphi^i_{C^-} = 0$	$\varepsilon^S_{11}, e_{15}$

$$u^\epsilon_i(x) = u^{(0)}_i(x) + \epsilon u^{(1)}_i(x,y) \tag{53}$$

$u^{(0)}_i$ is dependent only on x considering the lowest order BVD problem among the BVD problems in which the original BVD problem is split due to the AEH. This means that $u^{(0)}_i$ corresponds to the macroscopic displacement field of the homogenised material. From the second lowest order BVD problem it is possible to derive

$$u^{(1)}_i(x,y) = -\chi^{kl}_i(y)\frac{\partial u^{(0)}_k}{\partial x_l}(x) + \bar{u}^1_i \tag{54}$$

where $\bar{u}^1_i$ can be considered null [25]. Eq. (53) becomes:

$$u^\epsilon_i(x) = u^{(0)}_i(x) - \epsilon\chi^{kl}_i(y)\frac{\partial u^{(0)}_k}{\partial x_l}(x) \tag{55}$$

Eq. (55) must be differentiated according to Eq. (12) in order to find the expression of the strain fields:

$$\frac{\partial u^\epsilon_i(x)}{\partial x^\epsilon_j} = \frac{\partial u^{(0)}_i(x)}{\partial x_j} - \frac{\partial \chi^{kl}_i(y)}{\partial y_j}\frac{\partial u^{(0)}_k}{\partial x_l}(x) - \epsilon\chi^{kl}_i(y)\frac{\partial^2 u^{(0)}_k}{\partial x_l \partial x_j}(x) \tag{56}$$

The last term can be neglected because it is a second order derivative of the macroscopic displacement and the current analysis is restricted to linear strain. Therefore Eq. (56) can be rewritten as:

$$\frac{\partial u^\epsilon_i(x)}{\partial x^\epsilon_j} = \frac{\partial u^{(0)}_k(x)}{\partial x_l}\left(I^{ij}_{kl} - \frac{\partial \chi^{kl}_i(y)}{\partial y_j}\right) \tag{57}$$

Considering the properties of χ^{mn}_k stated above it is now clear that the strain field is different in the two phases only when $j = 2$. Therefore:

- S_1, S_3, S_5, E_1 and E_3 have the same values in both the phases.
- S_2, S_4, S_6 and E_2 are different between the two phases, but uniform inside each phase.

Stress fields and electric displacement fields, similarly, are uniform inside each phase. This means that for AEH in the case of the MFC has the same hypothesis of uniformity of the strain and stress fields inside each phase that is typical of the UFM. Moreover, the so called dependent and independent generalised strains in the UFM (see Section 4.1) are such also for the AEH. These are the reasons why the formula for the equivalent properties are the same for AEH and UFM in the case of MFCs. Eq. (57) provides an effective way to calculate the strain fields in the phases given the macroscopic strain fields.

5. Numerical periodic homogenisation

The numerical Periodic Homogenization Method (PHM) [10,14,16] is based on FEM analysis of the RVE. Using finite element analysis, it is possible to take into account the effect of electrodes and therefore results can be compared to the ones of AEH method. At the macroscale, MFCs can be defined as periodic repetition of RVEs (see Fig. 1). In order to take into account this repetition, periodic boundary conditions must be applied between opposite faces of the RVE. These boundary conditions are required to ensure the continuity of the generalised displacement (mechanical displacement and electric potential) through consecutive RVE models. In order to compute the values in the constitutive matrix of the homogeneous model a proper approach is to apply the periodic boundary condition in such a way that only one generalised average strain is different from zero. The corresponding column in the generalised stiffness matrix in Eq. (6) can be computed with the averaged values of the generalized stress components. The RVE has a parallelepiped geometry, see Fig. 1. Boundary conditions can be expressed more conveniently with reference to opposite faces of the RVE (A^- and A^+ are the opposite faces perpendicular to direction 1, B^- and B^+ to direction 2, C^- and C^+ to direction 3).

5.1. ABAQUS Implementation

The RVE is analysed using ABAQUS commercial finite element software. The RVE is discretised using 1300 8-node brick piezoelectric elements. The adopted mesh guarantees the convergence of at least three significant digits of the computed equivalent material properties. Mesh is uniform in order to have corresponding nodes

on opposite faces. Boundary condition are applied node to node thanks to the *Equation Constraint* feature available in ABAQUS. Table 2 presents a detailed description of the boundary conditions for each load case and the corresponding computed material coefficients. The magnitude of the jump between degrees of freedom of opposite nodes is null or have an arbitrary non-null value q depending on the load case. The equipotential conditions on the faces C^- and C^+ is enforced in order to consider the presence of the electrode. The equivalent coefficients are computed via simple ratios between average values, according to the load cases.

6. Results

The materials composing the MFC are epoxy matrix and piezoceramic SANOX P502 rectangular fibres. Epoxy is an isotropic material. Its properties are defined by the Young's modulus $E = 2.9$ GPa, the Poisson's ratio $\nu = 0.31$, and the relative permittivity $\varepsilon^s = 4.25$. The piezoceramic SONOX P502 is orthotropic with symmetry around the poling direction, which is direction 3. Its properties are defined in Table 3. d_{31}-type MFC has fibre volume fraction equal to 0.865.

6.1. Numerical validation using the PHM

The numerical results obtained using the AEH are compared with the analytical results obtained with formulae derived with the AEH and with the numerical PHM results. The effective values for the mechanical properties, the piezoelectric constants and the dielectric coefficients of the homogeneous MFC model are illustrated in Figs. 4–7. Analytical mixing rules, numerical AEH and PHM results match for almost every property. The only relevant difference is observed for G_{Tz} in the case of high volume fraction of the piezoelectric phase. The analytical solution is higher than the numerical solutions. This difference is due to the presence of the electrode. Indeed, the imposition of a uniform potential on the electrode surfaces causes the non-uniformity of some fields in the phases, invalidating the hypothesis of the UFM. In particular the electrodes cause a gradient of the electric potential along direction 3, E_3, and, because of the piezoelectric effect, local fields of S_1, S_2, S_3, T_1, T_2, T_3 arise at the interfaces between the two phases. Numerical AEH results take into account the effect of the electrodes and match results obtained with PHM. Predicted effective values obtained for MFC (fibre volume fraction equal to 0.865) with analytical solution, numerical AEH and PHM for mechanical properties, piezoelectric constants and dielectric coefficient are shown in Tables 4 and 5.

6.2. Experimental validations via manufacturer datasheets

The homogenised properties given by the AEH for the active layer, built of epoxy and PZT fibres, cannot be directly compared to the experimental values given by Smart Materials datasheets. In fact MFC is a laminate [29] where the active layer is intercalated between the electrodes (made of copper and epoxy) and kapton layers, as shown in Fig. 1. For the kapton layers, the following properties are used: $E = 2.8$ GPa, $\nu = 0.3$. For the electrode layers, the following properties are used: $E = 30.3$ GPa, $\nu = 0.31$. In-plane equivalent properties of the laminated sequence are computed on the basis of AEH results for the active layer with the Voigt mixing rule. The volume fractions are computed on the basis of layers thickness reported in the caption of Fig. 1. The free strain in longitudinal direction is computed as

$$S_L = d_{31}\frac{V}{h} \tag{58}$$

where V is the applied voltage and h is the thickness of the active layer. Table 6 presents a comparison between Smart Materials datasheets values and the computed results. Values are in close agreement.

7. Conclusion

The Asymptotic Expansion Homogenization method has been applied to the Macro Fiber Composite in order to compute the electro-elastic properties. An analytical solution is found neglecting the effect of electrodes. The obtained analytical mixing rules are the same as the ones obtained using the uniform field method through an automatic approach. In the case when the electrodes are taken into account, the AEH requires a numerical solution. The results obtained using Periodic Homogenization Method are used as a reference. A good agreement has been found. In-plane properties obtained using the numerical AEH method are compared with experimental results available from datasheets of the manufacturer.

Table 3
Piezoceramic SONOX P502 properties from CeramTec. ε_0 is the vacuum permittivity.

Properties	Symbol	Value
Young's modulus in GPa	$E_1 = E_2$	54.05
	E_3	48.30
Shear modulus in GPa	$G_{23} = G_{13}$	19.48
	G_{12}	19.14
Poisson's ratios	$\nu_{23} = \nu_{13}$	0.44
	ν_{12}	0.41
Piezoelectric charge constants in pC/N	$d_{31} = d_{32}$	−185
	d_{33}	440
	$d_{42} = d_{51}$	560
Dielectric relative constants	$\varepsilon^T_{11}/\varepsilon_0$, $\varepsilon^T_{22}/\varepsilon_0$	1950
	$\varepsilon^T_{11}/\varepsilon_0$	1850

Table 4
Computed mechanical properties for MFC with $\rho = 0.865$.

Mechanical properties	Mixing rules UFM/AEH	Numerical AEH	PHM
E_1 (GPa)	47.14	46.89	47.15
E_2 (GPa)	19.06	19.06	19.08
E_3 (GPa)	42.16	41.95	42.17
ν_{12}	0.3878	0.3880	0.3878
ν_{13}	0.4388	0.4387	0.4388
ν_{23}	0.1699	0.1704	0.1700
G_{12} (GPa)	6.011	6.015	6.015
G_{13} (GPa)	16.99	16.90	17.00
G_{23} (GPa)	6.664	6.216	6.216

Table 5
Computed electric and piezoelectric constants for MFC with $\rho = 0.865$.

Electromechanical properties	Mixing rules UFM/AEH	Numerical AEH	PHM
d_{31} (pC/N)	−182.9	−182.5	−182.9
d_{32} (pC/N)	−173.4	−173.0	−173.4
d_{33} (pC/N)	435.8	435.6	435.8
ε^S_{33} (nF/m)	6.068	6.039	6.069

Table 6
Numerical results and experimental values of MFC properties. MFC is considered globally, not only as its active layer.

Properties	Numerical AEH	Smart Materials datasheets
E_1 (GPa)	32.95	30.34
E_2 (GPa)	16.03	15.86
ν_{12}	0.35	0.31
S_L (10^{-6}/V)	1.01	1.1

Acknowledgments

This work has been developed in the context of the FNR MAFICOMECH Project (C08/MS/17). The authors acknowledge the financial support of Fonds National de la Recherche of Luxembourg (FNR).

Appendix A. Matrix based UFM in the case of MFC

In the case of MFC, provided that materials properties change along direction 2 (see Fig. 1), S_1, T_2, S_3, T_4, S_5, T_6, E_1, D_2 and E_3 are independent, whereas T_1, S_2, T_3, S_4, T_5, S_6, D_1, E_2 and D_3 are dependent. Following the procedure described in Section 4.2:

$$\mathbf{C}_{ID} = \begin{bmatrix} C^E_{22} & 0 & 0 & 0 \\ 0 & C^E_{44} & 0 & e_{24} \\ 0 & 0 & C^E_{66} & 0 \\ 0 & e_{24} & 0 & \varepsilon^T_{22} \end{bmatrix} \tag{A.1}$$

This matrix is invertible if its determinant:

$$C^E_{22}C^E_{66}(C^E_{44}\varepsilon^T_{22} - e^2_{24}) \neq 0 \tag{A.2}$$

The determinant is null only if $C^E_{44}\varepsilon^T_{22} = e^2_{24}$, being C^E_{22} and C^E_{66} not null.

References

[1] Hagood NW, Bent AA. Development of piezoelectric fiber composites for structural actuation. In: Collection of technical papers – AIAA/ASME structures, structural dynamics and materials conference. Pt 6. Massachusetts Inst of Technology, Cambridge, United States; 1993. p. 3625–38.
[2] Hagood NW, Kindel R, Ghandi K, Gaudenzi P. Improving transverse actuation of piezoceramics using interdigitated surface electrodes. In: Proceedings of SPIE, vol. 341; 1993.
[3] Bent AA, Hagood NW, Rodgers JP. Anisotropic actuation with piezoelectric fiber composites. J Intel Mater Syst Struct 1995;6(3):338.
[4] Bent AA, Hagood NW. Piezoelectric fiber composites with interdigitated electrodes. J Intel Mater Syst Struct 1997;8(11):903–19.
[5] Wilkie WK, Bryant RG, High JW, Fox RL, Hellbaum RF, Jalink Jr A, et al. Low-cost piezocomposite actuator for structural control applications. In: Proceedings of SPIE – the international society for optical engineering, vol. 3991. NASA Langley Research Cent, Hampton, United States; 2000. p. 323–34.
[6] Williams RB, Inman DJ, Schultz MR, Hyer MW, Wilkie WK. Nonlinear tensile and shear behavior of macro fiber composite actuators. J Compos Mater 2004;38(10):855–69.
[7] Williams RB, Inman DJ, Wilkie WK. Nonlinear response of the macro fiber composite actuator to monotonically increasing excitation voltage. J Intel Mater Syst Struct 2006;17(7):601–8.
[8] Tan P, Tong L. Micro-electromechanics models for piezoelectric-fiber-reinforced composite materials. Compos Sci Technol 2001;61(5):759–69.
[9] Tan P, Tong L. Investigation of loading assumptions on the effective electroelastic constants for PFRC materials. Compos Struct 2002;57(1–4):101–8.
[10] Berger H, Kari S, Gabbert U, Rodriguez-Ramos R, Bravo-Castillero J, Guinovart-Diaz R. A comprehensive numerical homogenisation technique for calculating effective coefficients of uniaxial piezoelectric fibre composites. Mater Sci Eng: A 2005;412(1–2):53–60.
[11] Tang T, Yu W. Variational asymptotic micromechanics modeling of heterogeneous piezoelectric materials. Mech Mater 2008;40(10):812–24.
[12] Oliveira JA, Pinho-da-Cruz J, Teixeira-Dias F. Asymptotic homogenisation in linear elasticity. Part II: finite element procedures and multiscale applications. Comput Mater Sci 2009;45(4):1081–96.
[13] Nasser H, Deraemaeker A, Belouettar S. Electric field distribution in macro fiber composite using interdigitated electrodes. Adv Mater Res 2008;47(1):1173–6 [Trans Tech Publ].
[14] Deraemaeker A, Nasser H, Benjeddou A, Preumont A. Mixing rules for the piezoelectric properties of macro fiber composites (MFC). J Intel Mater Syst Struct 2009.
[15] Deraemaeker A, Nasser H. Numerical evaluation of the equivalent properties of macro fiber composite (MFC) transducers using periodic homogenization. Int J Solids Struct 2010;47(24):3272–85.
[16] Berger H, Kurukuri S, Kari S, Gabbert U, Rodriguez-Ramos R, Bravo-Castillero J, et al. Numerical and analytical approaches for calculating the effective thermo-mechanical properties of three-phase composites. J Therm Stresses 2007;30(8):801–17.
[17] Benveniste Y. The determination of the elastic and electric fields in a piezoelectric inhomogeneity. J Appl Phys 1992;72(3):1086–95.
[18] Biao W. Three-dimensional analysis of an ellipsoidal inclusion in a piezoelectric material. Int J Solids Struct 1992;29(3):293–308.
[19] Eshelby J. The determination of the elastic field of an ellipsoidal inclusion, and related problems. Proc Roy Soc Lond Ser A: Math Phys Sci 1957;241(1226):376–96.
[20] Li JY. Thermoelastic behavior of composites with functionally graded interphase: a multi-inclusion model. Int J Solids Struct 2000;37(39):5579–97.
[21] Mori T, Tanaka K. Average stress in matrix and average elastic energy of materials with misfitting inclusions. Acta Metall 1973;21(5):571–4.
[22] Hill R. A self-consistent mechanics of composite materials. J Mech Phys Solids 1965;13(4):213–22.
[23] Koutsawa Y, Biscani F, Belouettar S, Nasser H, Carrera E. Multi-coating inhomogeneities approach for the effective thermo-electro-elastic properties of piezoelectric composite materials. Compos Struct 2010;92(4):964–72.
[24] Bravo-Castillero J, Guinovart-Diaz R, Sabina FJ, Rodriguez-Ramos R. Closed-form expressions for the effective coefficients of a fiber-reinforced composite with transversely isotropic constituents – II. Piezoelectric and square symmetry. Mech Mater 2001;33(4):237–48.
[25] Pinho-da-Cruz J, Oliveira JA, Teixeira-Dias F. Asymptotic homogenisation in linear elasticity. Part I: mathematical formulation and finite element modelling. Comput MaterSci 2009;45(4):1073–80.
[26] Guedes JM, Kikuchi N. Preprocessing and postprocessing for materials based on the homogenization method with adaptive finite element methods. Comput Methods Appl Mech Eng 1990;83(2):143–98.
[27] Bravo-Castillero J, Rodrguez-Ramos R. Homogenization of magneto-electro-elastic multilaminated materials. Quart J Mech Appl Math 2008; 61(3):311–32.
[28] Abaqus theory manual, version 6.5. Hibbit and Karlson and Sorensen Inc.; 2005.
[29] Williams RB. Nonlinear mechanical and actuation characterization of piezoceramic fiber composites. PhD thesis; 2004.